An Immunosensor Based on Hydrogen Evolution Signals of $CoNiSe_2$/g-C_3N_4 for Detection of Carcinoembryonic Antigen

Chunyu Yu [a], Lingfeng Gao [a] *, Shichen Wang [a], Haoqi Zhan [a], Long Wei [b], Zhibin Han [a], Zeyu Wang [a], Xu Sun [a] *, Qin Wei [a]

[a] School of Chemistry and Chemical Engineering, University of Jinan, Shandong, No.336 West Road of NanXinzhuang, Jinan 250022, China.

[b] Shandong China Recycling Resource Biotechnology Co. Ltd, No.1003, Futai Road, Taiping Town, Zoucheng City, Shandong Province.

* Corresponding author. E-mail addresses: chm_gaolf@ujn.edu.cn (Lingfeng Gao); chm_sunx@ujn.edu.cn (Xu Sun)

Table of contents

1. Chemical substances

Nickel chloride hexahydrate ($NiCl_2 \cdot 6H_2O$), Cobalt chloride hexahydrate ($CoCl_2 \cdot 6H_2O$), Selenium powder, Hydrazine Hydrate ($N_2H_4 \cdot H_2O$, 80 wt%), Melamine, Isopropanol, Chloroauric acid tetrahydrate ($HAuCl_4 \cdot 4H_2O$), Sodium citrate ($Na_3C_6H_5O_7 \cdot 2H_2O$), Sulfuric acid ($H_2SO_4$), Nafion were purchased from Aladdin. Ultrapure water (18.25 MΩ) was used throughout the entire experiment.

Carcinoembryonic antigen (CEA), Rabbit Anti-CEA (Monoclonal, Ab_1) and Mouse Anti-CEA (Polyclonal, Ab_2), Prostate-specific antigen (PSA), Procalcitonin (PCT), Human Serum Albumin (HSA), Immunoglobulin (IgG) and Neuron-Specific Enolase (NSE), Bovine Serum Albumin (BSA) were purchased from Beijing biosynthesis Co., Ltd. (Beijing, China). Phosphate buffer solution (PBS, 0.1 mol L^{-1}, pH = 7.4) is used as supporting electrolyte and dilution buffer. All chemical reagents are used directly without further treatment.

2. Characterization method

2.1. Instruments and equipment

The surface morphology and structure of the catalyst were studied using Gemini300 scanning electron microscope at a voltage of 10.0 kV. At the same time, in order to explore the internal structural characteristics, we used a transmission electron microscope for image acquisition. Use Rigaku Smart Lab to collect XRD patterns for analyzing crystal structure. Record 2θ Spectral information within the range of 20°to 80°. Using ESCALAB 250 electron spectrometer (American Thermo Fisher Scientific) and Al K α 150 W is used as an X-ray excitation source to record X-ray photoelectron spectroscopy (XPS). Perform elemental analysis on the catalyst using JEOLJSM-6700F EDS spectroscopy analysis. UV visible absorption spectra were obtained on the UV-3600 spectrometer. Infrared spectra were obtained on the VERTEX 70 Fourier transform infrared spectrometer. Finally, all electrochemical measurements were taken at the Shanghai Chenhua Electrochemical Workstation (CHI 760D).

2.2. Electrochemical measurements

The specific preparation method for the working electrode is as follows: Firstly, prepare a catalyst dispersion solution. Then take 5 mg of the catalyst and disperse it in 1 mL of Anhydrous Ethanol. After 1 h of ultrasonic treatment, acquire the catalyst

dispersion solution. Apply 8 μL of catalyst dispersed droplets to a polished glassy carbon electrode. After drying, they can be used as working electrodes.

The CHI 760D electrochemical workstation utilizes typical tri-electrode system which includes an altered glassy carbon electrode (GCE) as the working electrode, a SCE as the reference electrode and a platinum wire electrode as the counter electrode. Linear Sweep Voltammetry (LSV) was utilized to test HER in H_2SO_4 (0.1 mol L^{-1}) or PBS (0.1 mol L^{-1}). The Nyquist curve was recorded using Electrochemical Impedance Spectroscopy (EIS). Cyclic Voltammetry (CV) was employed to measure the double layer capacitance (C_{dl}) with different scan speeds (10, 20, 40, 80, 120 and 160 mV s^{-1}). The Tafel slope was estimated based on the LSV curve. Every measurement took place at ambient temperature, without infrared correction.

The construction process of electrochemical immunosensor was validated using CV and EIS in PBS. Simultaneously, perform HER (-1.5 V) chronoamperometry (*i-t*) for 100 s on the sensor for quantitative detection of CEA in PBS solution. Every measurement took place at ambient temperature.

3. LSV curves of $CoNiSe_2/g\text{-}C_3N_4$ with different $g\text{-}C_3N_4$ ratios

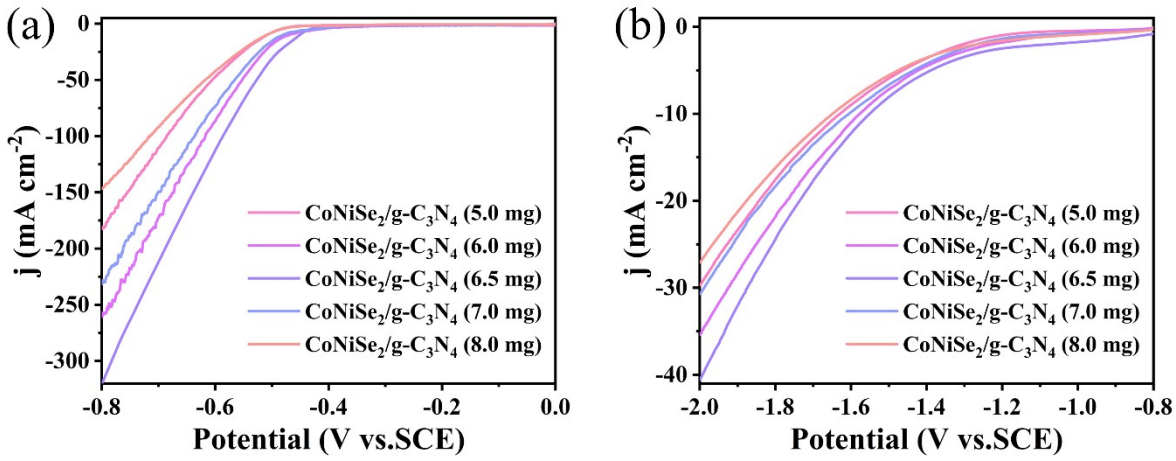

Fig. S1. The LSV curves of $CoNiSe_2/g\text{-}C_3N_4$ with different $g\text{-}C_3N_4$ ratios in (a) 0.5 mol L^{-1} H_2SO_4 and (b) 0.1 mol L^{-1} PBS.

4. XPS spectra of C 1s and N 1s from $CoNiSe_2/g\text{-}C_3N_4$

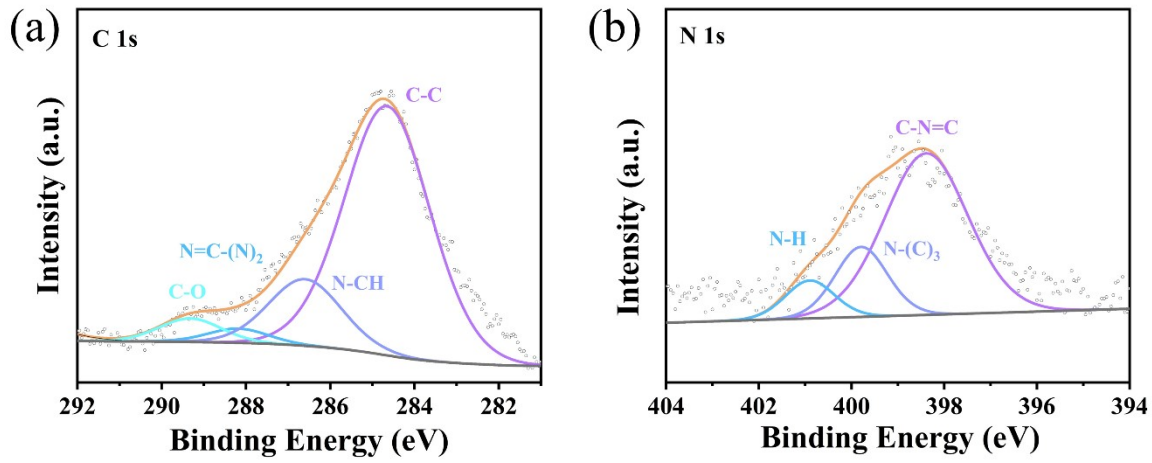

Fig. S2. XPS spectra of $CoNiSe_2/g\text{-}C_3N_4$, (a) C 1s spectrum and (b) N 1s spectrum.

5. XPS spectra of g-C_3N_4

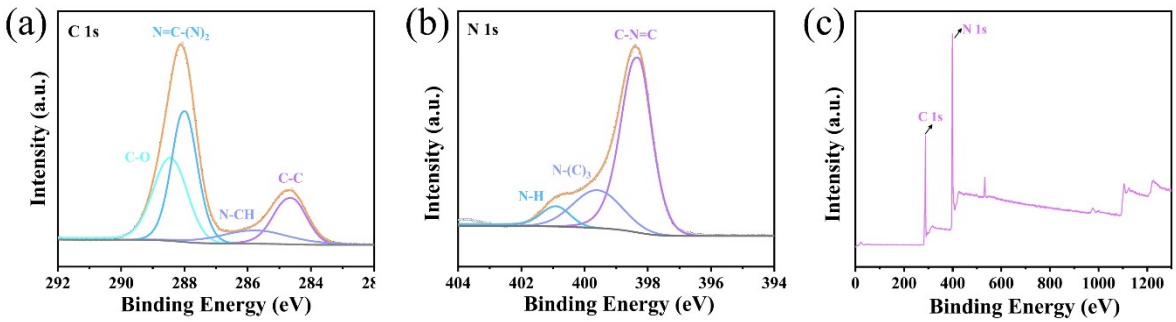

Fig. S3. XPS spectra of g-C_3N_4, (a) C 1s spectrum, (b) N 1s spectrum and (c) XPS survey spectrum.

6. XPS spectra of $CoNiSe_2$

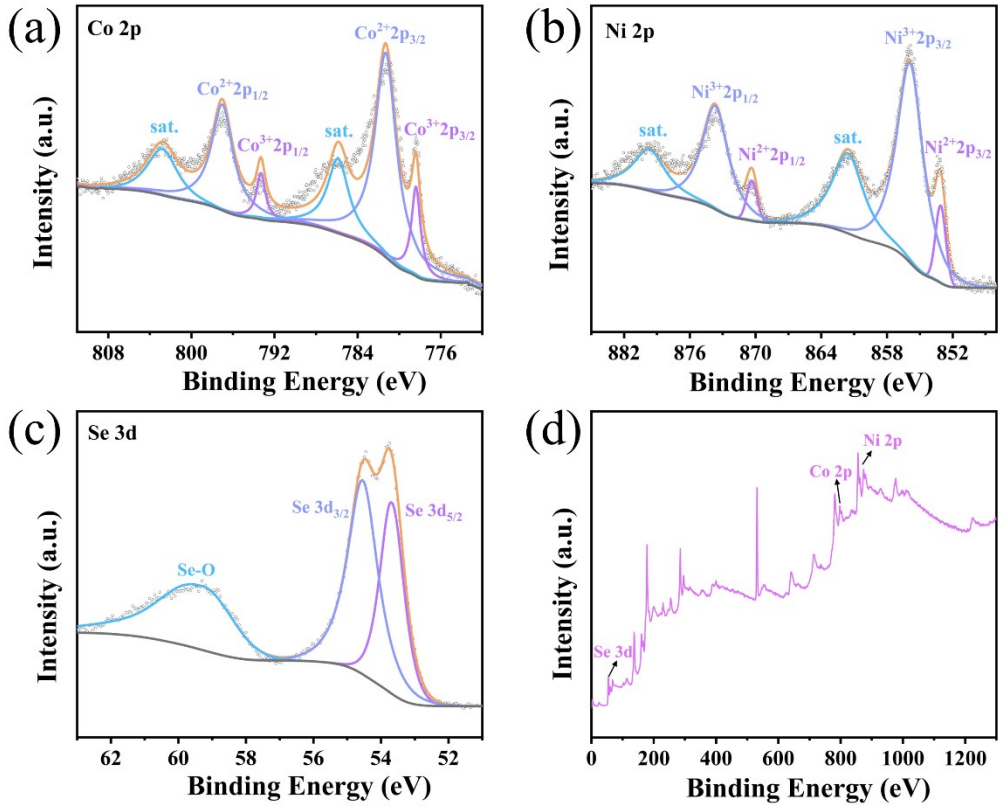

Fig. S4. XPS spectra of $CoNiSe_2$, (a) Co 2p spectrum, (b) Ni 2p spectrum, (c) Se 3d spectrum and (d) XPS survey spectrum.

7. SEM images of g-C_3N_4

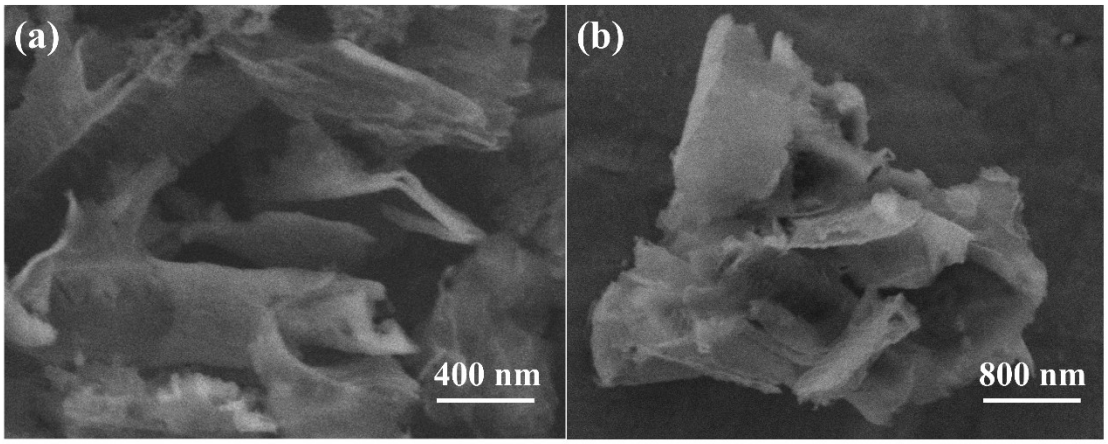

Fig. S5. SEM images of g-C_3N_4 (a) and (b).

8. HRTEM images of $CoNiSe_2$

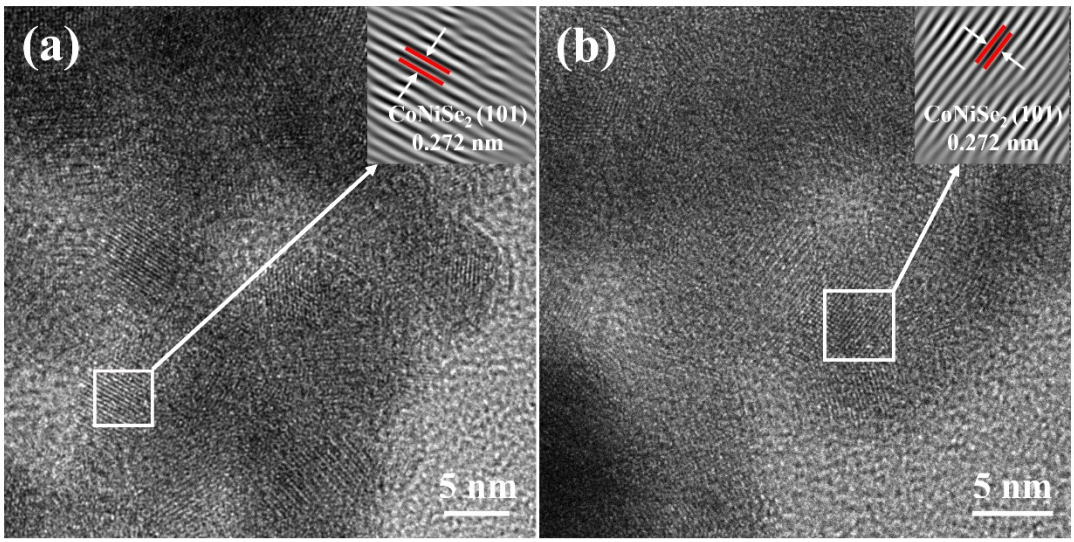

Fig. S6. HRTEM images of $CoNiSe_2$ (a) and (b).

9. CV curves of $CoNiSe_2$ and $CoNiSe_2$/g-C_3N_4

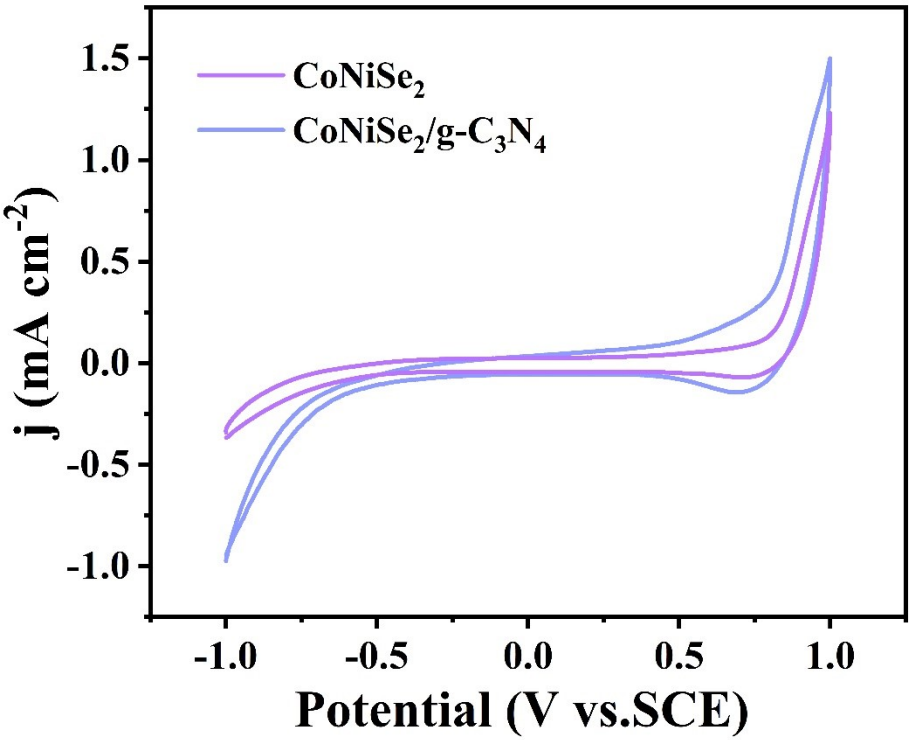

Fig. S7. The CV curves of $CoNiSe_2$/g-C_3N_4 and $CoNiSe_2$ in 0.1 mol L^{-1} PBS.

10. CV curves under different scan rates and values of C_{dl} in 0.1 mol L^{-1} PBS

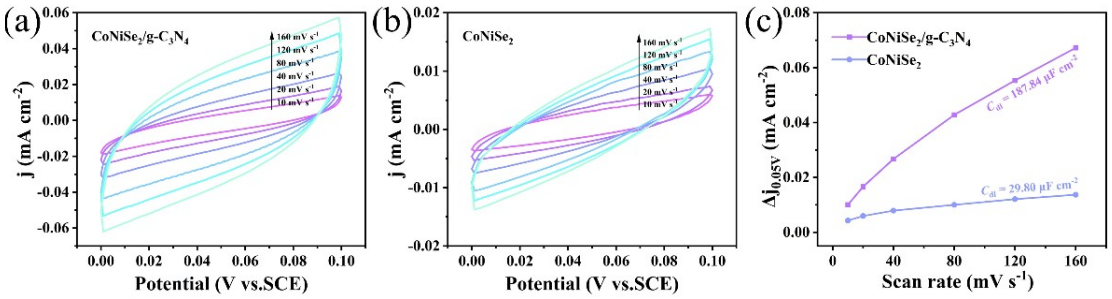

Fig. S8. The CV curves under different scan rates of $CoNiSe_2$/g-C_3N_4 (a) and $CoNiSe_2$ (b) in 0.1 mol L^{-1} PBS. (c) The C_{dl} values calculated based on (a) and (b).

11. Zeta-potential

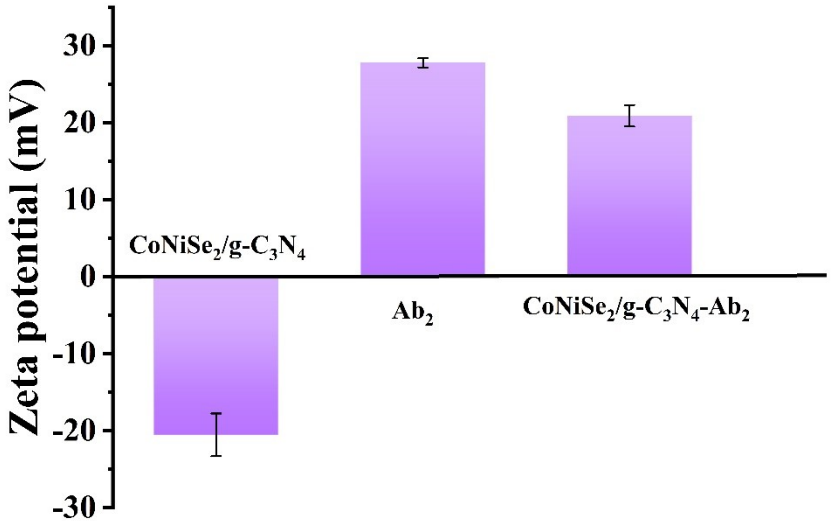

Fig. S9. Zeta-potential of $CoNiSe_2$/g-C_3N_4, Ab_2 and $CoNiSe_2$/g-C_3N_4-Ab_2.

12. Chronoamperometry test of different electrodes in 0.1 mol L^{-1} PBS

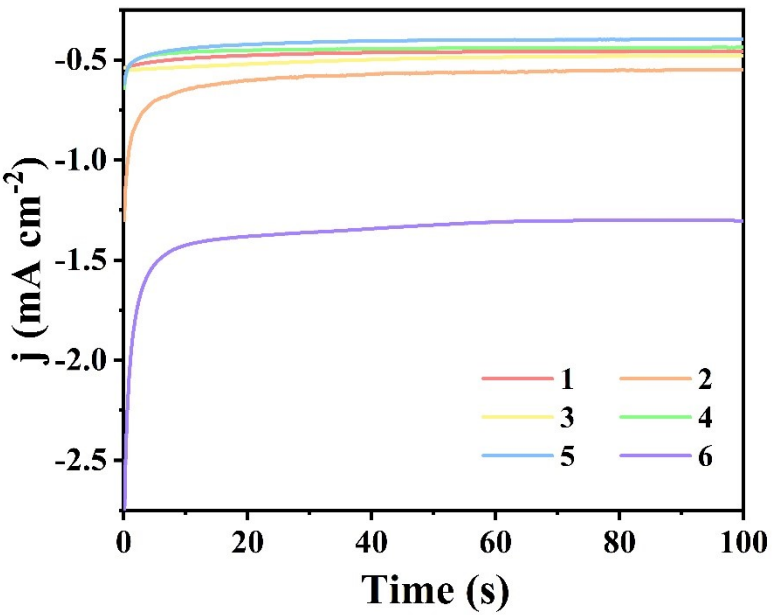

Fig. S10. *i-t* curves (-1.5 V) of different electrodes in 0.1 mol L^{-1} PBS. (1) GCE, (2) Au NPs/GCE, (3) Ab_1/Au NPs/GCE, (4) BSA/Ab_1/Au NPs/GCE, (5) CEA/BSA/Ab_1/Au NPs/GCE and (6) $CoNiSe_2$/g-C_3N_4-Ab_2/CEA/BSA/Ab_1/Au NPs/GCE.

13. LSV curve of the electrochemical immunosensor

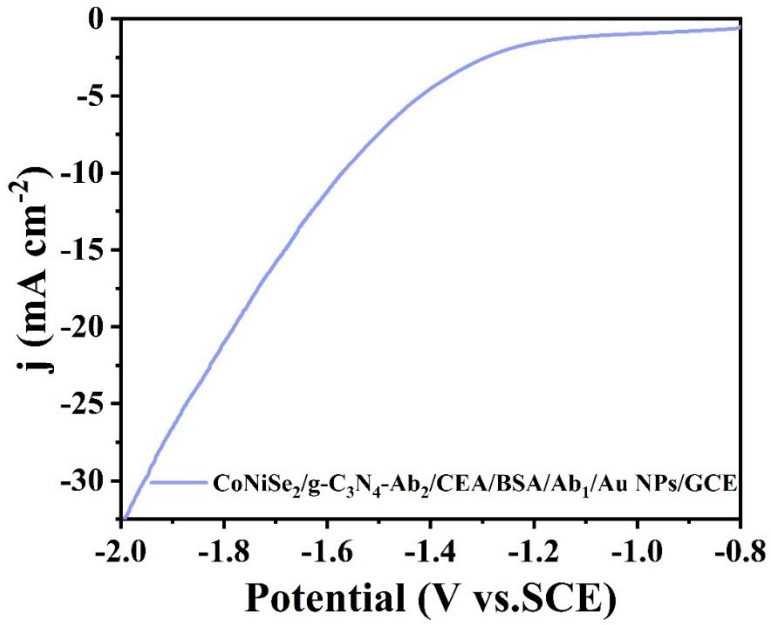

Fig. S11. The LSV curve of $CoNiSe_2$/g-C_3N_4-Ab_2/CEA/BSA/Ab_1/Au NPs/GCE in 0.1 mol L^{-1} PBS.

14. The optimization of construction time

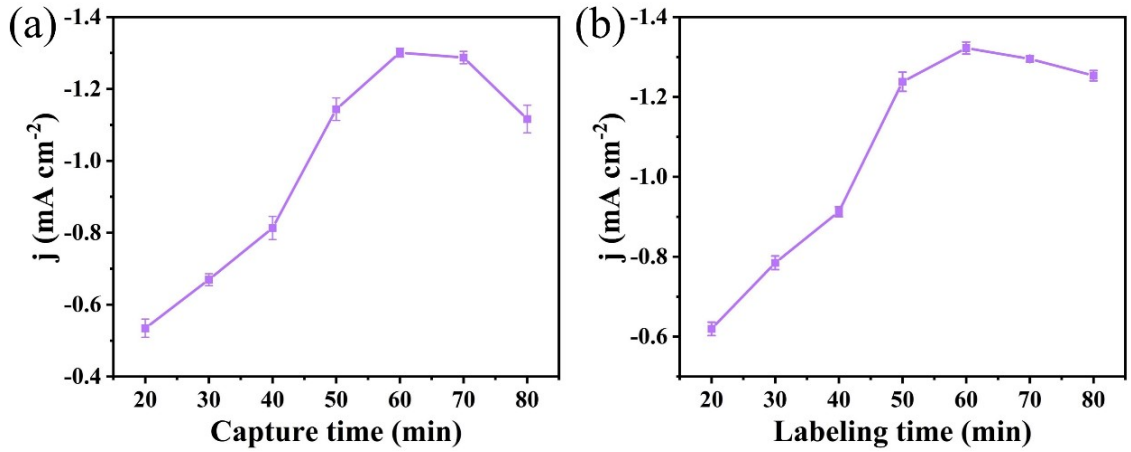

Fig. S12. The influence of capture time (a) and labeling time (b) on the HER current at -1.5 V in 0.1 mol L^{-1} PBS when 1 ng mL^{-1} CEA was detected. (error bar = SD, n = 3)

15. The optimization of voltage

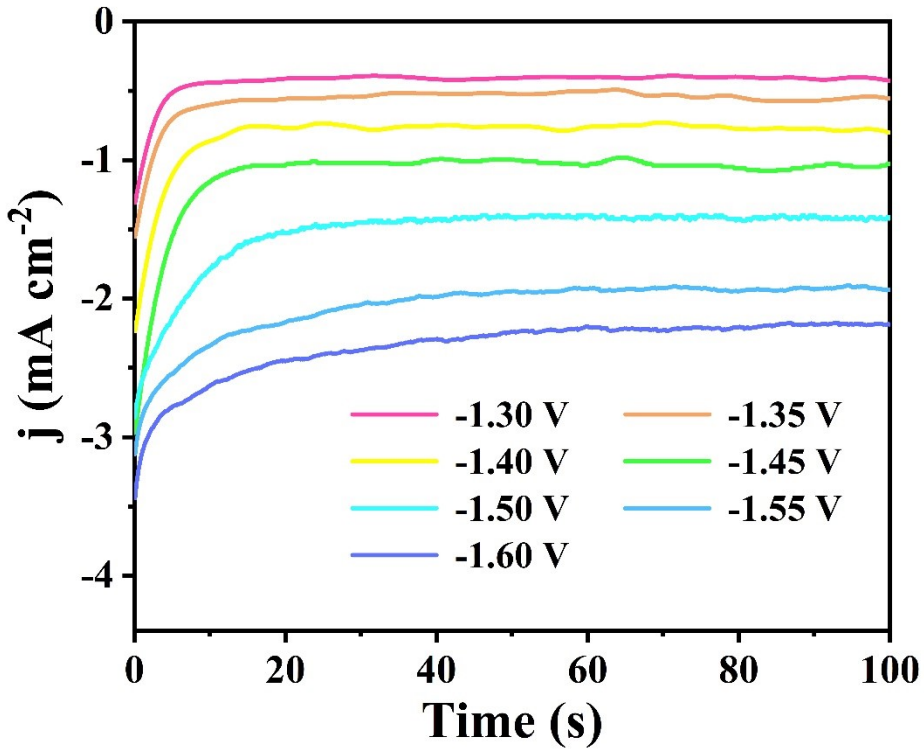

Fig. S13. The *i-t* curves of different voltages in 0.1 mol L^{-1} PBS.

16. Comparison of our immunosensor with other reported immunosensors

Table S1. Performance comparison of CEA detection with other electrochemical immunosensors in the literature[1-7].

Label	Linear range (ng mL^{-1})	Detection limit (ng mL^{-1})	References
Cu-CN/SPCE	0.01 - 50	0.0024	[1]
h-CdS/$CdMoO_4$	0.02 - 50	0.0113	[2]
Ferrocene Derivative	0.05 - 20	0.01	[3]
CeO_2-MoS_2-Pb^{2+}	0.001 - 80	0.0003	[4]
Mercapto-amine functionalised receptor	1 - 100	0.33	[5]
MWCNT-NH_2 supported PdPt nanocages	0.001 - 20	0.0002	[6]
Au/Pt DNs/NG/Cu^{2+}	500 - 50	167	[7]
$CoNiSe_2$/g-C_3N_4	0.0001 - 100	0.00018	This work

Table S2. Performance comparison of CEA detection with other analytical methods in the literature[8-13].

Technique	Linear range (ng mL^{-1})	Detection limit (ng mL^{-1})	References
Colorimetry	0.5 - 100	0.013	[8]
Enzyme-linked immunosorbent assay	0.01 - 0.5	0.01	[9]
Fluorescence immunoassay	0.5 - 128	0.1	[10]
Surface plasmon resonance	0.01 - 10	0.3	[11]
Surface enhanced Raman spectroscopy	1 - 50	0.1	[12]
Chemiluminescence immunoassay	0.05 - 500	4.53×10^{-3}	[13]
Electrochemical immunoassay	0.0001 - 100	0.00018	This work

Supplementary References

1. C. Q. Huang, Y. N. Li, F. Cai, H. B. Zhong, F. L. Zhang, W. M. Zhong, L. Yao and J. Y. Huang, *New J. Chem.*, 2023, **47**, 12117-12122.
2. L. J. Chi, X. Y. Wang, H. Y. Chen, D. P. Tang and F. Q. Xue, *Talanta*, 2023, **254**, 8.
3. X. F. Gu, Z. She, T. X. Ma, S. Tian and H. B. Kraatz, *Biosens. Bioelectron.*, 2018, **102**, 610-616.
4. W. J. Li, X. W. Qiao, C. L. Hong, C. Y. Ma and Y. J. Song, *Anal. Biochem.*, 2020, **592**, 8.
5. M. Pavithra, S. Muruganand and C. Parthiban, *Sens. Actuator B-Chem.*, 2018, **257**, 496-503.
6. N. Li, Y. G. Wang, W. Cao, Y. H. Zhang, T. Yan, B. Du and Q. Wei, *J. Mat. Chem. B*, 2015, **3**, 2006-2011.
7. H. Lv, Y. Y. Li, X. B. Zhang, Z. Q. Gao, C. Y. Zhang, S. Zhang and Y. H. Dong, *Biosens. Bioelectron.*, 2018, **112**, 1-7.
8. X. Li, J. L. Huang, J. Y. Ding, M. Z. Xiu, K. Huang, K. Cui, J. Zhang, S. J. Hao, Y. Zhang, J. H. Yu and Y. Z. Huang, *Biosens.-Basel*, 2023, **13**, 15.
9. H. Y. Yan, L. Jiao, H. J. Wang, W. Q. Xu, Y. Wu, W. L. Gu, D. Du, Y. H. Lin and C. Z. Zhu, *Sens. Actuator B-Chem.*, 2019, **297**, 7.
10. L. H. Ding, X. Chen, L. L. He, F. Yu, S. C. Yu, J. Wang, Y. M. Tian, Y. L. Wang, Y. J. Wu, L. E. Liu and L. B. Qu, *Microchim. Acta*, 2020, **187**, 8.
11. C. P. Guo, F. F. Su, Y. P. Song, B. Hu, M. H. Wang, L. H. He, D. L. Peng and Z. H. Zhang, *ACS Appl. Mater. Interfaces*, 2017, **9**, 41188-41199.
12. Y. Lin, G. H. Xu, F. D. Wei, A. X. Zhang, J. Yang and Q. Hu, *J. Pharm. Biomed. Anal.*, 2016, **121**, 135-140.
13. Y. A. Hou, J. D. Wang, S. T. Liu, Y. L. Sun, Y. X. Dai, C. N. Luo and X. Y. Wang, *Talanta*, 2023, **253**, 7.